Journal of Food Engineering 188 (2016) 87–97

Contents lists available at ScienceDirect

Journal of Food Engineering

journal homepage: www.elsevier.com/locate/jfoodeng

Analysis of electric field distribution within a microwave assisted thermal sterilization (MATS) system by computer simulation

Donglei Luan [a, 1], Juming Tang [a, *], Patrick D. Pedrow [b], Frank Liu [a], Zhongwei Tang [a]

[a] Department of Biological Systems Engineering, Washington State University, P. O. Box-646120, Pullman, WA 99164-6120, USA
[b] School of Electrical Engineering and Computer Science, Washington State University, P.O. Box-642752, Pullman, WA 99164-2752, USA

ARTICLE INFO

Article history:
Received 24 August 2015
Received in revised form
26 April 2016
Accepted 11 May 2016
Available online 13 May 2016

Keywords:
Microwave heating
Computer simulation
Propagation mode
Waveguide wavelength
Phase shift
Electric field distribution

ABSTRACT

Microwave heating holds potential to improve food quality of low acid shelf-stable or chilled meals as compared to conventional thermal processes. Several thermal processes based on pilot-scale 915 MHz single-mode microwave assisted thermal sterilization (MATS) systems have received acceptances from regulatory agencies in USA. In this study a comprehensive computer simulation model was developed to study microwave distributions within waveguides and applicators of the MATS system. A three-dimensional model was developed based on Maxwell equations using the finite difference time-domain method. It was validated and then used to analyze electric field distribution in different parts of the MATS waveguide configuration and in a microwave heating cavity. Simulation results indicated that the TE10 mode was consistent within the waveguide elements. The dominant electric field component within the microwave heating cavity controlled the heating pattern in the food packages. Adjusting the dimension of the cavity in the dominant direction should help improve heating uniformity. Food packages immerged in water reduced the edge heating of packaged foods. Adjusting the phase of standing wave within the microwave heating cavity can improve the heating uniformity in the direction of the thickness. The information from this study should assist design of industrial systems with improved heating uniformity in food packages.

1. Introduction

A 915 MHz single model microwave assisted thermal sterilization (MATS) system was developed at Washington State University, Pullman, WA, USA, to explore industrial applications of microwave volumetric heating in thermal processing of pre-packaged foods (Tang et al., 2006, 2008). It was also used for developing knowledges and collecting data for regulatory filing and industrial scale-up. In October 2009, a filing for a MATS process of prepackaged mashed potato was accepted by the US Food and Drug Administration (FDA). This marked the first FDA accepted microwave process for sterilization of pre-packaged low acid food in the United States. Since then, two additional processes were accepted by FDA, one in 2011 (salmon fillet) at Washington State University and another in 2014 (mashed potato) at AmeriQual Foods, Evansville, IN. A non-objection letter was received from US Department of Agriculture Food Safety and Inspection Services (USDA FSIS) for microwave sterilization and pasteurization of shelf-stable or chilled foods containing more than 2% meat, poultry or egg products (Tang, 2015). These successes have generated great confidence and interest for scaled-up systems used in industrial production.

A MATS system consists of four sections: preheating, microwave heating, holding and cooling, which represents four steps of an industrial process (Resurrection et al., 2013). Each of these four sections had a separated water circulation system with different temperature settings. Packaged foods are immerged in water bed and transported through MATS system via a conveyor belt. In the preheating section, packaged foods are equilibrated to a uniform initial temperature. They are then moved through interconnected microwave cavities in the microwave heating section and heated to a target temperature (i.e. 121 °C) for sterilization. The food packages continue moving in hot water of 123 °C through holding section to achieve designed thermal lethality. The residence times for each package in the microwave heating and holding sections are

* Corresponding author.
E-mail address: jtang@wsu.edu (J. Tang).
[1] Current address: Engineering Research Center of Food Thermal-processing Technology, Department of Food Science and Technology, Shanghai Ocean University, Shanghai, China.

http://dx.doi.org/10.1016/j.jfoodeng.2016.05.009
0260-8774/

between 3 and 5 min depending on product formulation and thickness of the food package. The packages are then moved into a cold water section for cooling to room temperature. The design of the microwave applicators in the microwave heating section determines heating uniformity and processing time and, thus, is one of the most important parts of a MATS system. In support of process filing to FDA, computer simulation models were developed to assist design of microwave applicators (Pathak et al., 2003), and to predict and study stability of heating patterns in packages foods in MATS systems (Chen et al., 2007; Resurrection et al., 2013, 2015). Simulation models were also used to support determination of cold spots in food packages by chemical markers (Chen et al., 2008; Resurrection et al., 2013, 2015; Lau et al., 2003; Pandit et al., 2007) and to analyze interference of microwave intensity on accuracy of temperature measurement by mobile metallic temperature sensors (Luan et al., 2013, 2015). All those studies only considered MATS cavities in the simulation models, without considering waveguide configurations that connected microwave cavities to 915 MHz generators. There is a need to develop a more comprehensive simulation model to study microwave standing waves within the complete waveguide system to reveal how waveguide and applicator design could influence heating uniformity.

A major challenge in scaling-up the MATS system is the non-uniform heating pattern caused by the uneven electric field distribution. Hot and cold spots occur at locations of high and low electric field intensity, respectively. The non-uniform heating can be severer when using high microwave power in industrial scale MATS systems. It is because microwave energy absorbed by food is proportional to the square of the electric field intensity. Furthermore the dielectric loss factor of food materials in general increases with increasing temperatures (Datta, 2001). Hence, the temperature difference between the hot spot and cold spot will continuously increase as long as high microwave power is applied. This type of non-uniform heating affects the selection of thermal process parameters. Thus, a systematic analyses of the electric field distribution and the formation of heating pattern within the complete MATS system will provide the fundamental information for improving heating uniformity and guidelines for designing industrial systems.

The objective of this study was to analyze microwave propagation mode and electric field distribution inside the MATS system through numerical simulation. These results could give insight into the dominating factors that control electric field pattern in the MATS system and provide guidelines for designing MATS systems in industrial scale.

2. Theories

2.1. Electromagnetic wave and governing equations

Microwaves are electromagnetic (EM) waves within a frequency range of 300 MHz to 300 GHz (Decareau, 1985). EM waves have two components: electric field component ($\vec{E}$) and magnetic field component ($\vec{H}$). These two components are vector quantities that have both magnitude and direction. EM wave is a transverse wave. That is, the directions of field components are perpendicular to the propagating direction of energy and wave. The traveling EM waves are governed by the Maxwell's equations. The differential form of Maxwell's equations describe and relate the electric and magnetic field vectors, current and charge densities at any point in space at any time. The differential forms of Maxwell's equations are shown below (Balanis, 1989):

$$\nabla \times \vec{E} = -\frac{\partial \vec{B}}{\partial t} = -\mu \frac{\partial \vec{H}}{\partial t} \tag{1-a}$$

$$\nabla \times \vec{H} = \sigma \vec{E} + \frac{\partial \vec{D}}{\partial t} = \vec{J} + \varepsilon \frac{\partial \vec{E}}{\partial t} \tag{1-b}$$

$$\nabla \cdot \vec{D} = \rho \tag{1-c}$$

$$\nabla \cdot \vec{B} = 0 \tag{1-d}$$

where $\vec{E}$ is electric field intensity, $\vec{D}$ is electric flux density, $\vec{H}$ is the magnetic field intensity, $\vec{B}$ is magnetic flux density, $\vec{J}$ is volume current density. Some of the above variables are related as $\vec{B} = \mu \vec{H}\, \vec{D} = \varepsilon \vec{E}$, $\vec{J} = \sigma \vec{E}$. Each of the variables is a function of space coordinates and time, for example, $\vec{E} = \vec{E}(x, y, z; t)$. *The variable* ρ is the volume charge density. The constitutive parameters ε, μ and σ are permittivity, permeability and conductivity, respectively; they are the electric and magnetic properties of the material. In free space, the values of permittivity and permeability are $\varepsilon_0 = 10^{-9}/(36\pi)$ F/m and $\mu_0 = 4\pi \times 10^{-7}$ H/m, respectively. The conductivity in free space is zero.

2.2. Boundary conditions

The differential form of Maxwell's equations is valid where the field vectors are continuous functions of position and time and these functions have continuous derivatives. Along the boundaries where the electrical properties of the two media are not continuous, the field vectors are also discontinuous. The boundary conditions describe these vectors' behavior across the interface of the two media (medium 1 and medium 2) with different electrical properties:

$$\hat{n} \times \left(\vec{E}_2 - \vec{E}_1\right) = 0 \tag{2-a}$$

$$\hat{n} \times \left(\vec{H}_2 - \vec{H}_1\right) = \vec{J}_s \tag{2-b}$$

$$\hat{n} \cdot \left(\vec{D}_2 - \vec{D}_1\right) = q_s \tag{2-c}$$

$$\hat{n} \cdot \left(\vec{B}_2 - \vec{B}_1\right) = 0 \tag{2-d}$$

where $\vec{J}_s$ is the induced electric current density due to the existence of electrical charges; q_s is the surface charge density at the boundary plane. Eqs. (2a–d) are the general form of boundary conditions which can be modified for different media. If the two media are both dielectric materials without electrical charges and have constitutive parameters of ε_1, μ_1, σ_1 and ε_2, μ_2, σ_2, respectively, the boundary condition can be written as:

$$\hat{n} \times \left(\vec{E}_2 - \vec{E}_1\right) = 0 \tag{3-a}$$

$$\hat{n} \times \left(\vec{H}_2 - \vec{H}_1\right) = 0 \tag{3-b}$$

$$\hat{n}\cdot\left(\vec{D}_2-\vec{D}_1\right)=\hat{n}\cdot\left(\varepsilon_2\vec{E}_2-\varepsilon_1\vec{E}_1\right)=0 \tag{3-c}$$

$$\hat{n}\cdot\left(\vec{B}_2-\vec{B}_1\right)=\hat{n}\cdot\left(\mu_2\vec{H}_2-\mu_1\vec{H}_1\right)=0 \tag{3-d}$$

Eqs. (3-a) and (3-b) indicate that the tangential component of electric and magnetic field intensity across the interface is continuous; Eqs. (3-c) and (3-d) indicate that the normal component of electric and magnetic flux density across the surface is continuous. The normal component of electric and magnetic field intensity is, however, not continuous.

2.3. Propagation mode in rectangular waveguide

The propagation modes of microwaves within a metallic waveguide are the results of possible solutions of the wave equations that satisfy the boundary conditions. Within a rectangular waveguide, assuming that the microwave propagation direction is along z axis (Fig. 1A), the following three configurations can be obtained from the solutions of wave equations (Dibben, 2001):

transverse electromagnetic (TEM^z): components of both electric and magnetic fields in the propagation (z) direction are equal to zero, $Hz = Ez = 0$.

transverse magnetic (TM^z): the magnetic field component in the propagation (z) direction is equal to zero, $Hz = 0$.

transverse electric (TE^z): the electric field has no component in the propagation (z) direction, $Ez = 0$.

However, the TEM^z mode does not satisfy the boundary condition of the waveguide wall. Fig. 1A illustrates the dimension of a rectangular waveguide that transmitting EM energy in positive z direction. Considering a TE^z mode as an example, the solutions of EM waves in this waveguide are (Balanis, 1989):

$$E_x^+=A_{mn}\frac{\beta_y}{\varepsilon}\cos(\beta_x x)sin\left(\beta_y y\right)e^{-j\beta z} \tag{4-a}$$

$$E_y^+=-A_{mn}\frac{\beta_x}{\varepsilon}\sin(\beta_x x)cos\left(\beta_y y\right)e^{-j\beta_z z} \tag{4-b}$$

$$E_z^+=0 \tag{4-c}$$

$$H_x^+=A_{mn}\frac{\beta_x\beta_z}{\omega\mu\varepsilon}\sin(\beta_x x)cos\left(\beta_y y\right)e^{-j\beta_z z} \tag{4-d}$$

$$H_y^+=A_{mn}\frac{\beta_y\beta_z}{\omega\mu\varepsilon}\cos(\beta_x x)sin\left(\beta_y y\right)e^{-j\beta_z z} \tag{4-e}$$

$$H_z^+=-jA_{mn}\frac{\beta_x^2+\beta_y^2}{\omega\mu\varepsilon}\cos(\beta_x x)cos\left(\beta_y y\right)e^{-j\beta_z z} \tag{4-f}$$

In which

$$\beta_x^2+\beta_y^2+\beta_z^2=\beta^2=\omega^2\mu\varepsilon \tag{5-a}$$

$$\beta_x=\frac{m\pi}{a} \tag{5-b}$$

$$\beta_y=\frac{n\pi}{b} \tag{5-c}$$

where E_x^+, E_y^+, E_z^+, H_x^+, H_y^+ and H_z^+ represent the electric and magnetic field intensity in each component within the rectangular coordinate system; the superscript (+) indicates that the EM wave is propagating in +z direction; β_x, β_y and β_z are the components of phase constant β in each coordinate direction; a and b represent the dimensions of the waveguide in x and y directions; m and n are integer numbers which are not zero at the same time in a solution ($m \neq n = 0, 1, 2, \ldots$); A_{mn} is the amplitude constant of the solution corresponding with m and n. From physical standpoint, the propagating EM wave (in z direction) forms standing waves in x and y directions. The integer number m and n indicates the number of semi-sinusoidal variations (anti-node) in the x and y direction, respectively. Fig. 2 displays the electric field distributions for some TE modes with different semi-sinusoidal combinations (m and n).

Solution with different values of m and n leads to different modes. With a given mode, there is a matching cutoff frequency (f_c) for each type of waveguide. The EM wave cannot propagate within the waveguide if its frequency is lower than the cutoff frequency. The cutoff frequency could be derived from:

$$(f_c)_{mn}=\frac{1}{2\pi\sqrt{\mu\varepsilon}}\sqrt{\left(\frac{m\pi}{a}\right)^2+\left(\frac{n\pi}{b}\right)^2} \tag{6}$$

In a waveguide, the transmitted microwave mode with lowest frequency is called the dominant mode. The dominant TE10 mode is always the normal operation mode of a rectangular waveguide for power transmission (Fig. 1B).

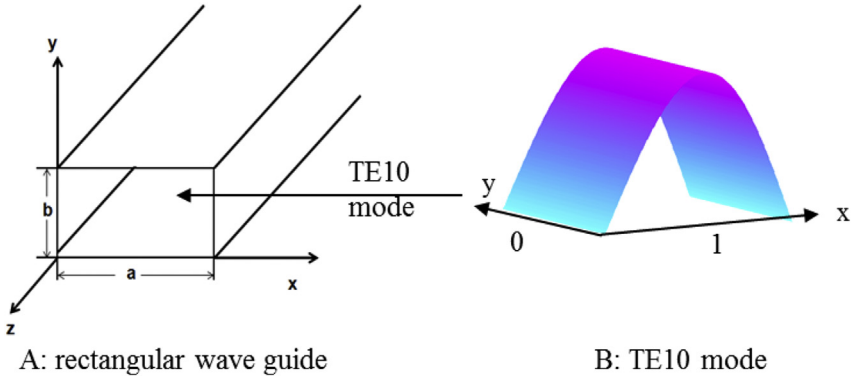

Fig. 1. Rectangular waveguide (A) and its dominant mode (B). For TE10 mode, Ez = 0, Ex = 0. The electric field component in y direction (Ey) formed a standing wave in x direction with one semi-sinusoidal variation.

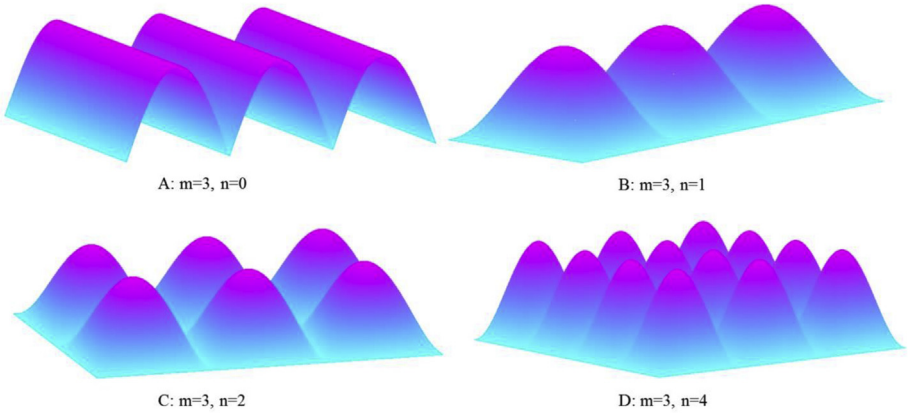

Fig. 2. Electric field distribution of some TEmn modes: A: $m = 3$, $n = 0$; B: $m = 3$, $n = 1$; C: $m = 3$, $n = 2$; D: $m = 3$, $n = 4$.

3. Methodology

3.1. Physical model

The MATS system installed at Washington State University consists of four sections, i.e. preheating, microwave heating, holding and cooling. The packaged foods are transported through these four sections in sequence by a microwave transparent conveyor belt that immersed in a thin bed (76 mm) of circulating water. Each section has its own water circulating system with different settings of water temperature. The structure of MATS system and the detailed operation process was described by Resurrection et al. (2013). Among these four sections, the microwave heating section is the key element in reducing processing time and improving food quality.

The microwave heating section contains four connected microwave heating cavities. Fig. 3 shows a typical microwave heating cavity and the attached waveguide elements through which microwave power is delivered from the generator to the heating cavity. Each cavity has two windows (top and bottom) made from a high temperature resistant polymer (Ultem® 1000). Microwaves are delivered to the heating cavity through the Ultem windows that are connected to two identical horn shaped applicators on the top and bottom. The horn applicator is a tapered shape parallelogram with wide end connected to the window and narrow end connected to a standard WR975 waveguide element that having an inner cross sectional dimension of 247.7 mm by 123.8 mm.

A tee junction is used to split the microwave power equally to the top and bottom horn applicators. On the bottom two connected E-bend waveguides direct the microwave to the narrow end of the horn applicator. On the top, two short waveguides are used to connect E-bend with horn applicator and tee-junction. These two short waveguides are installed for phase adjustment. Several standard WR975 rectangular waveguide elements are used to connect the generator and the tee-junction including an H-bend waveguide. The E-bend or H-bend waveguide is used to change the propagating direction of microwaves. In Fig. 3, an H-bend waveguide is shown to change the microwave propagating from x to y direction.

3.2. Computer simulation model for electric field distribution analysis

Computer simulation model was developed using the commercial software QuickWave version 7.5 (QW3D, Warsaw, Poland) based on the physical model of the MATS system and finite difference time domain (FDTD) method. The mesh size in different materials was set following the rules of more than ten cells per wavelength (Rattanadecho, 2006). The metal wall was assumed as perfect electric conductor (PEC). The dielectric and thermal

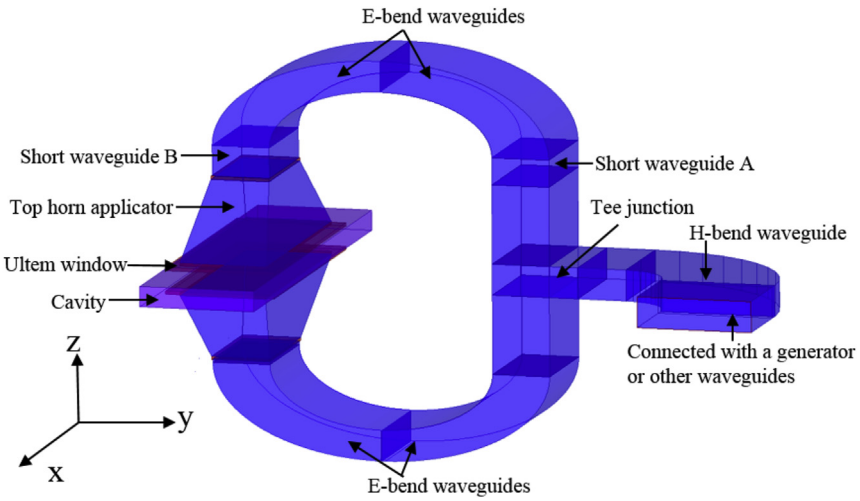

Fig. 3. Microwave heating cavity and waveguide assembly.

properties of water and food were updated with changing temperatures, the detailed data were reported in Resurrection et al. (2013). Only one microwave heating cavity with attached waveguide elements was built up in this study (Fig. 3) to analyze the microwave propagation mode and electric field component distribution from waveguide to the microwave heating cavity.

A sinusoidal microwave source with TE10 mode was set at the port. In a rectangular waveguide with a lateral dimensions a and b ($a > b$), as shown in Fig. 1A, the dominant propagation mode of electromagnetic (EM) wave was TE10 mode. The symbol TE indicated that the electric field component was perpendicular to the propagation direction (i.e. z direction in Fig. 1A). The symbols 1 and 0 in a mode type denoted the number of semi-sinusoidal variations in x and y direction, respectively (Fig. 1B). For a TE10 mode propagating in the coordinate system described in Fig. 1A, the electric field had no component in z (Ez) and x (Ex) directions. The component in y direction (Ey) formed a standing wave in x direction with one semi-sinusoidal variation.

The numerical method and steps of developing a simulation model based on the software of QuickWave have been described in detail in previous studies (Resurrection et al., 2013; Luan et al., 2013, 2015). This study focused on utilizing the validated model to analyze the electric field distribution within the waveguide elements and the microwave heating cavity.

3.3. Experimental validation

The heating pattern obtained from experimental test via MATS system was used to validate the computer simulation model. Preformed whey protein gel (WPG, 95 × 140 × 16 mm^3) containing 75.4% water, 23.3% protein, 1% D-ribose and 0.3% salt was utilized as model food in the experimental test. The procedure described by Wang et al. (2009) in preparing WPG was used. The detailed operation process for experimental validation was reported by Resurrection et al. (2013). Chemical marker (M-2) method and computer vision method (Lau et al., 2003; Pandit et al., 2007) were applied to obtain the heating pattern of food. The production of M-2 was irreversible and dependent on accumulated effect of time and temperature. Thus, the intensities of brown color (color of M-2) represented the heating treatment pattern of WPG. The original heating pattern showing brown color distribution was processed by computer vision method to create a heating pattern in pseudo color (Fig. 4A). In this study, only the temperature distribution, which represents the electric field distribution, was concerned (Fig. 4B).

4. Results and discussion

4.1. Validation of the computer simulation model

The experimental and simulation results for heating patterns of food in top view (x-y plane) in the middle layer in z direction are shown in Fig. 4. Similar heating patterns were observed between experimental and simulation results, which verified that the simulation model was reliable. Thus, the predicated propagation of microwave from the port, through the waveguide, horn shape applicator to the microwave heating cavity was reliable.

4.2. Electric field distribution in waveguides

Natural biological materials, such as food, interact with only the electric part of the electromagnetic field (Mudgett, 1986). Thus electric field distribution is of the most concern. Fig. 5 shows the simulated distribution of the overall electric field (i.e. the norm of the electric field) and its Ey component within the microwave heating system. They were snapshots of side views (y-z plane) at the middle layer of x direction (Fig. 3).

In Fig. 5A, the simulated overall electric field distribution was clearly presented as wave crests and troughs. The distance between two wave crests was equal to half waveguide wavelength. It was around 223.5–227.8 mm which was much longer than that of 915 MHz microwave in free space (i.e. 163.9 mm of half wavelength).

Propagation of microwave in waveguide is different from that in free space (Balanis, 1989; Dibben, 2001). The EM waves in a rectangular waveguide can be depicted as a sum of two plane TEM waves propagating along zigzag path between the waveguide walls in x direction (Fig. 6). The EM wave component in z direction has a different wavelength from that of the plane waves. The wavelength along the axis of the waveguide is called the waveguide wavelength. Waveguide wavelength is given by (Sadiku, 2007):

$$\lambda_g = \frac{\lambda_0}{\sqrt{1-(f_c/f)^2}} \tag{7}$$

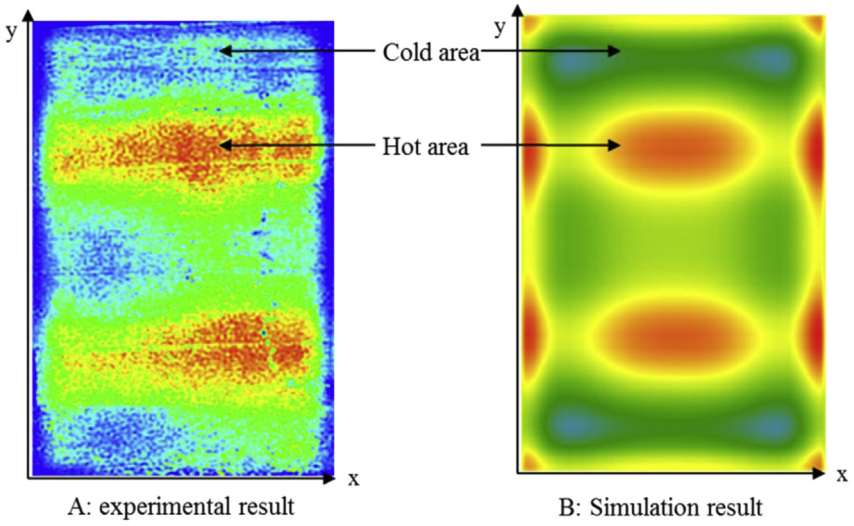

Fig. 4. Heating pattern comparison between (A) experimental result and (B) simulation result. The dimension of whey protein gel was 95 × 140 × 16 mm^3.

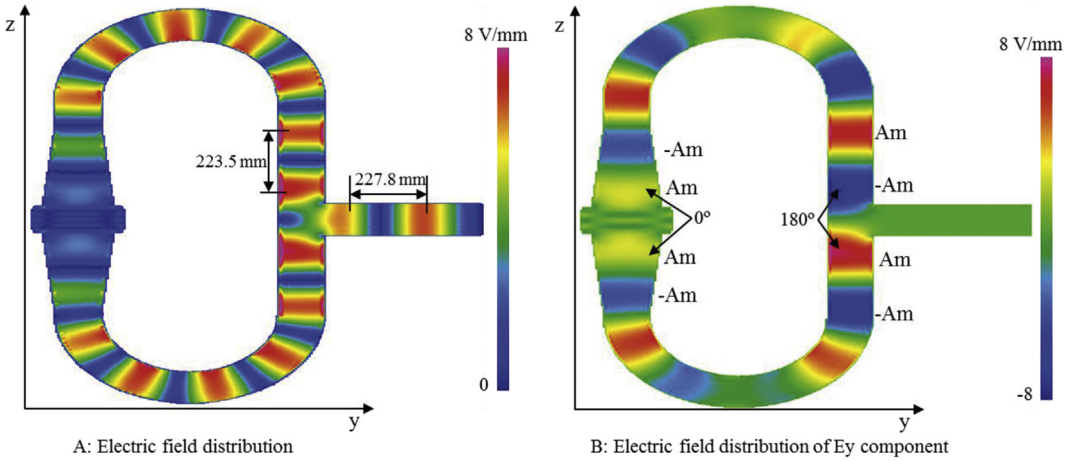

Fig. 5. Snapshots of field propagation in side view for A: overall electric field distribution; B: electric field distribution in y direction, i.e. Ey component, Am stands for amplitude.

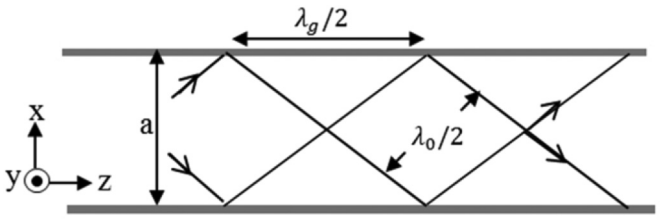

Fig. 6. Waveguide wavelength of microwaves within a rectangular waveguide.

In which, f and λ_0 is the microwave frequency and wavelength in free space, f_c is cutoff frequency. For a TE10 mode in a rectangular waveguide with dimensions of a and b ($a > b$), the formula for calculating waveguide wavelength is simplified to:

$$\lambda_g = \frac{\lambda_0}{\sqrt{1-(\lambda_0/2a)^2}} \tag{8}$$

From Eq. (8), the waveguide wavelength is larger than that of a plane wave with the same frequency. For 915 MHz microwave, the theoretical waveguide wavelength is 218.7 mm following Eq. (8), which is close to the simulation result shown in Fig. 5. Knowing the value of waveguide wavelength is very important in accurately adjusting the microwave propagating phase in waveguide design.

It is shown in Fig. 5B that there was a 180° phase difference when microwaves propagating through the tee-junction. To remove the phase difference caused by the tee-junction, two short waveguides, each of which had a length of quarter waveguide wavelength, were applied (Fig. 3). As a result, zero phase difference was observed between the two microwaves that propagated to the microwave heating cavity from top and bottom horn applicators (Fig. 5B). More information for adjusting phase shift is described in Section 4.3.

The electric field components in different cross sections were analyzed to reveal the propagation mode within the waveguide system that includes H-bend, E-bend and tee-junction. Fig. 7 summarizes the snapshots of electric field distributions and the field components in each direction at the microwave source port and selected cross sections within the waveguide. Cross section 1 is located at the interface between the H-bend and the tee-junction. Cross section 2a and 2b are located at the beginning of E-bends. At the connection of the two E-bend elements are the cross section 3a and 3b. Cross section 4a and 4b are selected at the interface between the waveguides and the horn applicators.

Results indicated that the microwave propagation mode (i.e. TE10 mode) was consistent. There was only one dominant electric field component along the narrow side of the waveguide cross section. It is reasonable that the cross section of the standard WR975 waveguide is consistent. Thus, theoretically the propagation mode or electric field distribution at different cross sections should be the same. However, the dominant electric field component may shift while changing the microwave propagation direction.

From Eqs. (3a–b), the component of the electric field parallel to the surface of the load created much higher field intensity and, consequently higher power density within the load, than a component of electric field with equal strength but normal to the surface (Dibben, 2001). Thus, the direction of the dominant electric field component should be designed using different waveguide components to ensure that it was parallel to the largest surface of the food package.

4.3. Electric field distribution in horn applicator and microwave heating cavity

Not all the waveguide elements were essential in a computer simulation model since they had no influence on the propagation mode of the microwaves. The dimension of the physical model was significantly reduced by removing most of the waveguide elements to save the computer memory and calculation time. Fig. 8 shows a simplified model with only two short waveguides, horn applicators and the microwave heating cavity. In this model, the microwave source port was set 200 mm higher than the horn applicator to provide sufficient long waveguide for reference plane of the microwave source. The reference plane of the microwave source should be at least 150 mm distance from the port.

With two sinusoidal microwave sources at top and bottom of the simplified model in Fig. 8, the snapshots of electric field distribution in front view (x-z plane, middle layer in y direction) and side view (y-z plane, middle layer in x direction) are illustrated in Fig. 9. The TE10 propagation mode is clearly shown from the front view and side view within the waveguide. As shown in Fig. 9A, the electric field intensity had one semi-sinusoidal variation in x direction. Uniform electric field intensity was observed in y direction (Fig. 9B). The half waveguide wavelength of microwave propagating between waveguide and horn applicator reduced to 195.5–198.6 mm, which was shorter than that within waveguide (Fig. 5). This is because the dimension of horn applicator was larger

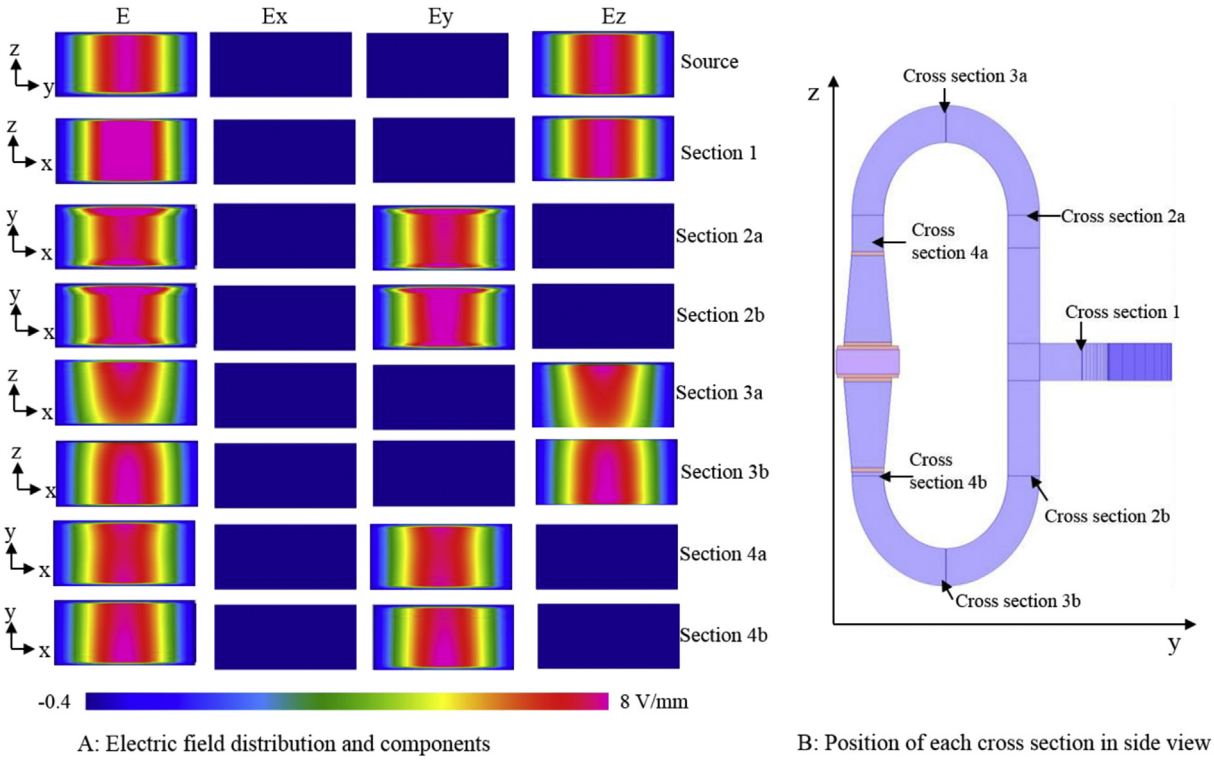

Fig. 7. Snapshots of electric field distribution and intensity of each field component at different cross sections of the waveguide. A: Electric field distribution and intensity of different field components; B: position of each cross section in the side view of microwave heating cavity and attached waveguides.

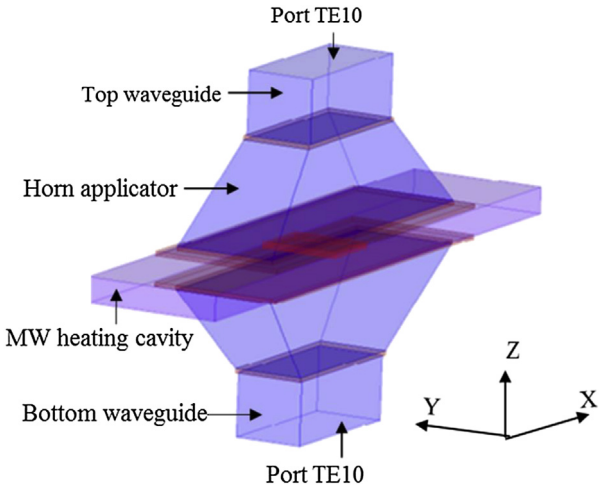

Fig. 8. Microwave heating cavity with only horn applicators and short waveguides.

than that of waveguide. From Eq. (8), a larger dimension of waveguide leads to a shorter waveguide wavelength.

There are three standing wave nodes within the microwave heating cavity in the z direction. The distance between the first and second anti-node is 22.4 mm. This is the half wavelength of 915 MHz microwave in water. The wavelength in dielectric materials is reduced to $1/\sqrt{\varepsilon_r}$ of that in free space, where ε_r is the relative permittivity of the dielectric material (Wappling-Raaholt et al., 2002). The wavelength shift from air to water is clearly demonstrated in Fig. 9B. The theoretically calculated wavelength of 915 MHz microwave in water (with dielectric constant of 55.8 at 122 °C) is 22.1 mm. Results indicate that in microwave heating cavity the waveguide wavelength predicted by computer simulation is very close to the theoretically calculated one and that the predicted result from computer simulation is reliable.

Besides waveguide wavelength, the electric field distribution changes with the increasing dimension of the horn applicator. The electric field distribution within the horn applicator and the microwave heating cavity is not a standard TE10 mode any more. Snapshots of overall electric field distribution and each field component in the x-y plane at different cross sections are shown in Fig. 10A. Marked by the red double head arrows, cross sections T1 and B1 are located at the wave crest of the microwave snapshot within the waveguides. Cross sections T2 and B2 are at the adjacent wave crest within the horn applicators. At the open ends of the horn applicators are cross sections T3 and B3. Cross section M is located at the middle of the microwave heating cavity.

Fig. 10B shows electric field distributions and field components at different cross sections. From the waveguide to the microwave heating cavity, the dominant electric field component was consistent (i.e. Ey). However, when microwaves propagated through the horn applicator, the electric field distribution in y direction is not as uniform as it was in the waveguide, especially near the edge of the horn applicator. Furthermore, at the middle of the microwave heating cavity, staggered electric field intensity is observed in the y direction (section M in Fig. 10B). Possible reason for this type of electric field distribution is the abrupt dimension variation from the horn applicator to the microwave heating cavity. From the point of view of heating uniformity, a rectangular applicator providing TE20 or TE30 mode for the microwave heating cavity is recommended.

Electric field distribution determines the heating pattern of the food loads. However, the presence of food may also affect the electric field distribution. Snapshots of the electric field distribution without food and with food at the center of the microwave heating cavity are shown in Fig. 11. Ey is the dominant electric field component at the middle layer of the microwave heating cavity.

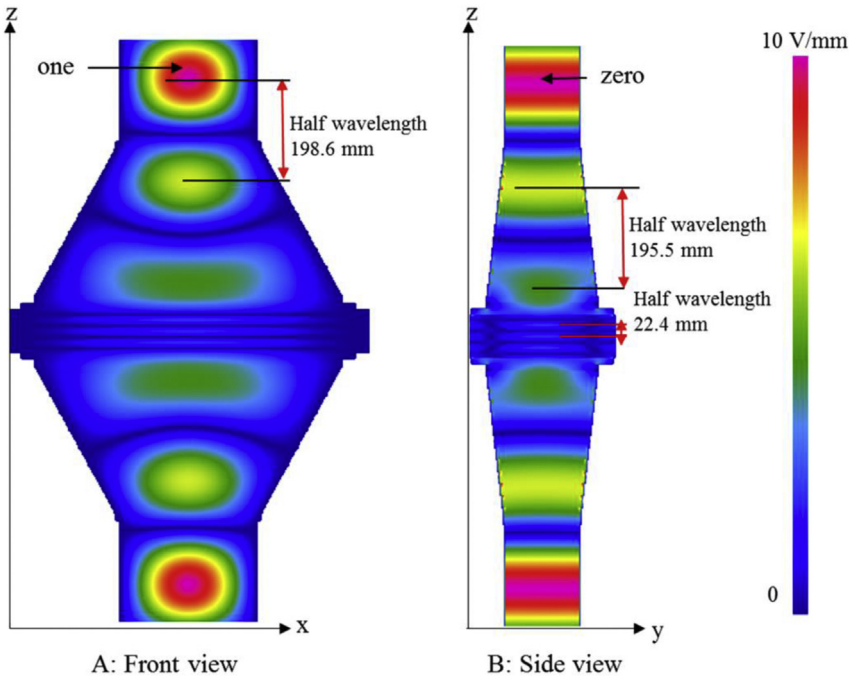

Fig. 9. Snapshots of electric field distribution. A: front view, x-z plane, middle layer in y direction, one semi-sinusoidal variation in x direction. B: side view, y-z plane, middle layer in x direction, zero semi-sinusoidal variation in y direction.

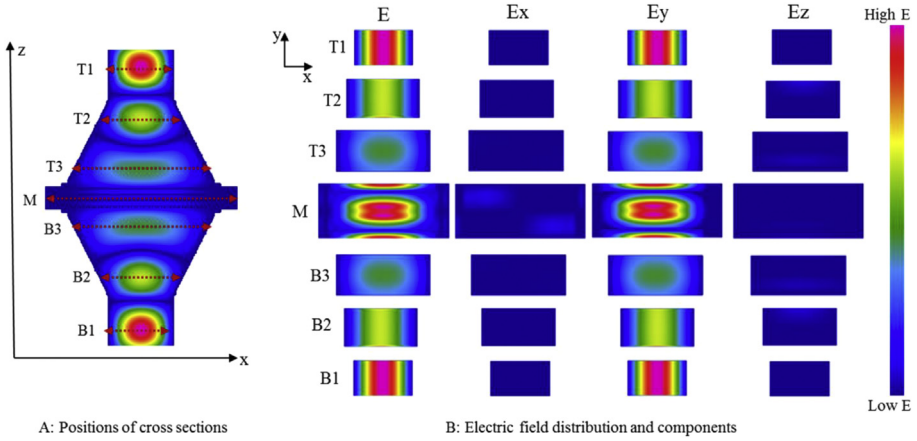

Fig. 10. Snapshots of electric field distribution and each component within the cross section of x-y planes.

The electric field distribution within food is similar to that in the cavity without food load, i.e. there are two high electric field intensity bands in y direction. But the continuity of the electric field distribution in x direction is cut off by the presence of food. Non-uniform heating pattern is due to the uneven electric field distribution of Ey component in y direction. A uniform design of the electric field distribution in y direction is the proper solution to obtain good heating patterns. The electric field distribution can be changed by adjusting the dimension of the cavity in y direction, while current MATS system using Ultem wall to obtain different heating patterns within four microwave heating cavities (Resurrection et al., 2013).

4.4. Phase shift and wavelength shift

MATS system was designed to ensure that the microwaves propagating from the top and bottom of the microwave heating cavities have zero phase difference. Standing waves formed within the microwave heating cavity in z direction. An anti-node exists at the middle of the microwave heating cavity in z direction. The electric field component distribution in Fig. 5B reveals that the phase difference (180°) caused by tee-junction is removed through adjusting the waveguide length. Applying this technique, 90° and 180° phase differences were simulated by adding a short waveguide at the top of the simplified model in length of quarter and half waveguide wavelength, respectively. Fig. 12 shows the overall electric field intensity at the center of each x-y plane.

A node and antinode arose at the middle of the microwave heating cavity (i.e. position = 0 mm in Fig. 12) for 180° and 0° phase difference, respectively. However, for 90° phase difference, neither node nor anti-node was observed at the middle position. Fig. 13 shows the intensity of each electric field component. It clearly revealed the phase difference during wave propagation. Results shows that by proper phase adjustment, the electric field intensity

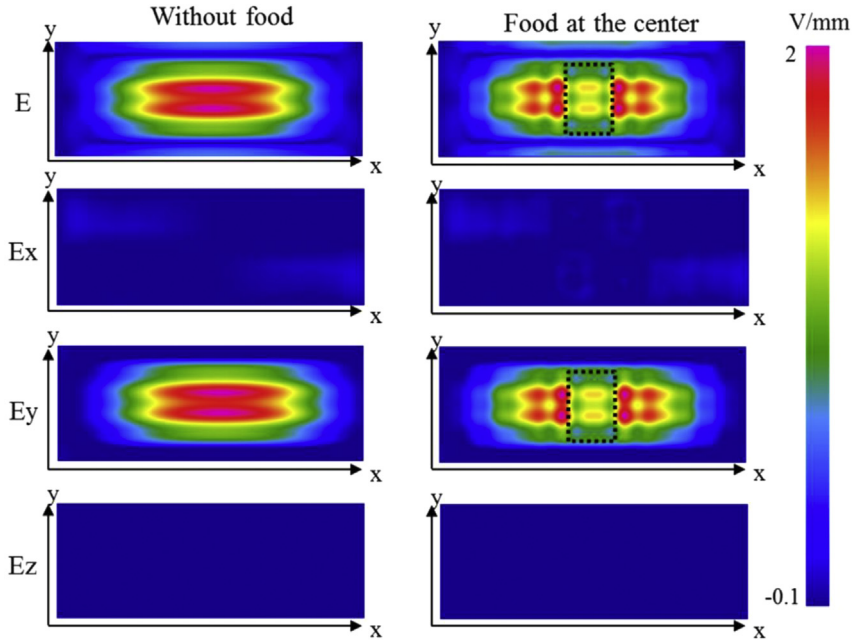

Fig. 11. Snapshots of electric field distribution and components in each direction at the middle layer of the microwave heating cavity. The results for the cavity without food load and the cavity with food load are listed at the left column and right column, respectively.

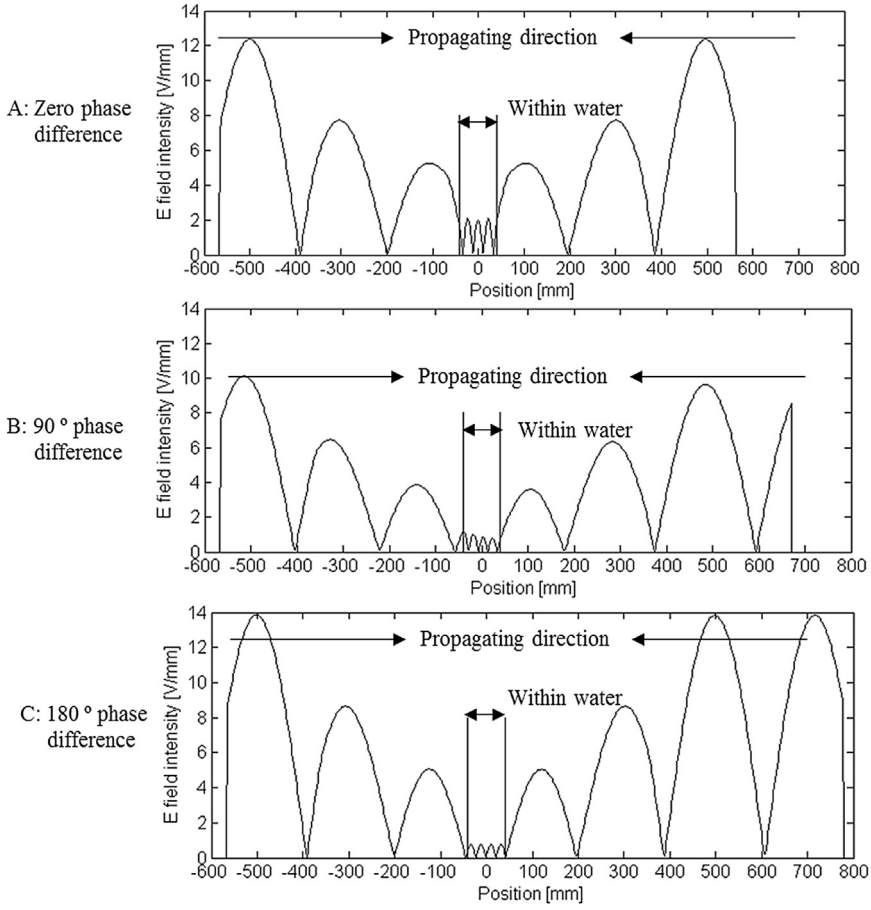

Fig. 12. Propagation in the z direction of overall electric field at the center of x-y plane. A: zero phase difference, B: 90° phase difference, C: 180° phase difference.

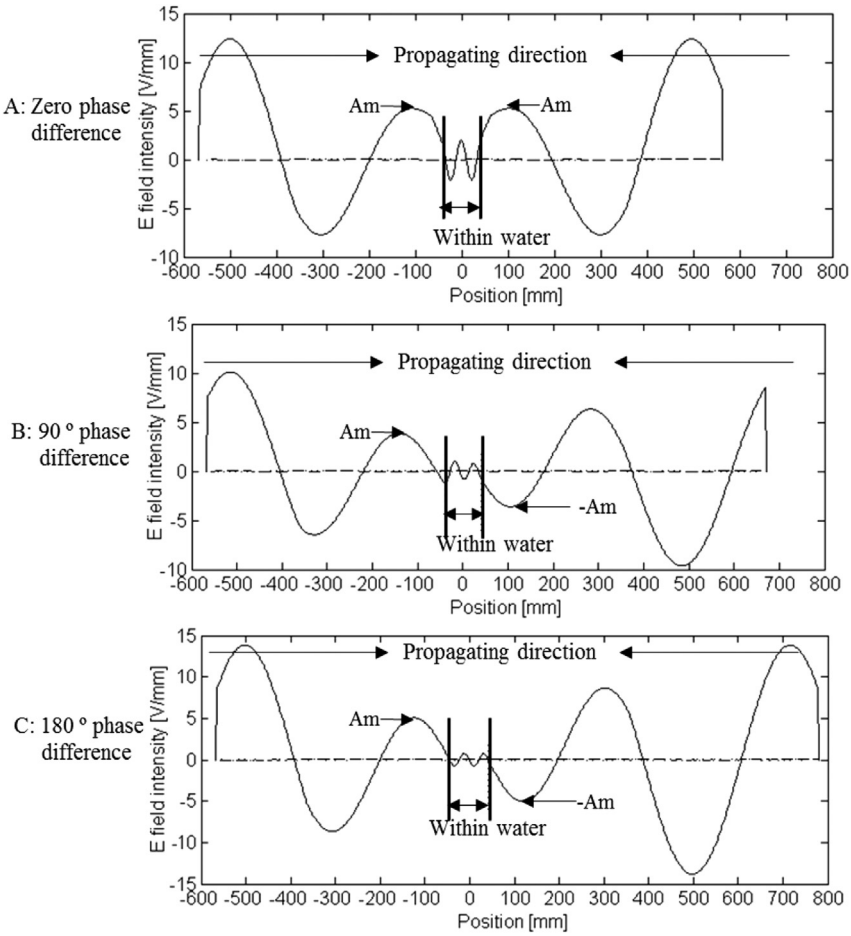

Fig. 13. Propagation in the z direction of electric field components at the center of the x-y plane, Ex·····, Ey——, Ez– – –. A: zero phase difference, B: 90° phase difference, C: 180° phase difference.

at the middle of the microwave heating cavity can be adjusted between maximum (anti-node) and minimum (node). The heating uniformity in z (thickness) direction of the food load can be adjusted through this type of phase shift.

Same as electric field components shown in Fig. 10B, Ey is the dominant component during the propagation in z direction. Furthermore, the reduction of wavelength and electric field intensity in water was observed. Because from Eqs. (3c–d), for the electric field normal to the food load surface, the field intensity decreases to $1/\sqrt{\varepsilon_r}$ from air to the load, where ε_r is the relative permittivity of a food load. For high moisture foods, the value of ε_r varies between 40 and 80 depending upon food composition and temperature (Sosa-Morales et al., 2010). This is one of the reasons for edge heating when a food is heated in a domestic microwave oven. Thus it is a good design for the MATS system to reduce edge heating by immersing packaged food in water during microwave heating process, as discussed in Tang (2015).

5. Conclusions

The microwave propagation and electric field distribution within the MATS system was studied using computer simulation to reveal the design principles. The TE10 propagation mode of microwave is consistent throughout all the waveguide elements. There is only one dominant electric field component within the waveguide along the narrow side of the rectangular waveguide. The superposition of two microwaves from top and bottom of the microwave heating cavity forms a standing wave in z direction. Within the horn applicator and microwave heating cavity, the electric field component in y direction (Ey) is the dominant electric field component which determined the heating pattern. However, the electric field distribution in y direction changes with the changing dimensions. Thus, the heating uniformity in y direction can be improved by adjusting the dimension of microwave heating cavity in y direction.

The waveguide wavelength in rectangular waveguide was verified numerically using theoretical calculations. The theory of waveguide wavelength can be used to adjust the phase of standing waves within a microwave heating cavity for improving heating uniformity in the thickness direction of a food package. Besides waveguide wavelength, a much shorter microwave wavelength and much lower electric field intensity was observed within water due to the high electric permittivity of water. This type of electric field intensity shift is the major reason for edge heating in air. The water bed design in the MATS system effectively reduced the edge heating.

Acknowledgements

This project was supported by the Agriculture and Food Research Initiative of the USDA National Institute of Food and Agriculture, grant number #2011-68003-20096, and partially Washington State University Agricultural Center. The authors also thank the Chinese Scholarship Council for providing a scholarship to Donglei Luan for his Ph.D. studies at WSU.

References

Balanis, C.A., 1989. Advanced Engineering Electromagnetics. John Wiley, New York.

Chen, H., Tang, J., Liu, F., 2007. Coupled simulation of an electromagnetic heating process using the finite difference time domain method. J. Microw. Power Electromagn. Energy 41 (3), 50–68.

Chen, H., Tang, J., Liu, F., 2008. Simulation model for moving food packages in microwave heating processes using conformal FDTD method. J. Food Eng. 88, 294–305.

Datta, A.K., 2001. Fundamentals of heat and moisture transport for Microwaveable food product and process development. In: Datta, A.K., Anantheswaran, R.C. (Eds.), Handbook of Microwave Technology for Food Applications. CRC Press, Boca Raton, FL, pp. 115–172.

Decareau, R.V., 1985. Microwaves in the Food Processing Industry. Academic Press, Inc., New York.

Dibben, D., 2001. Electromagnetics: fundamental aspects and numerical modeling. In: Datta, A.K., Anantheswaran, R.C. (Eds.), Handbook of Microwave Technology for Food Applications. CRC Press, Boca Raton, FL, pp. 1–28.

Lau, M.H., Tang, J., Taub, I.A., Yang, T.C.S., Edwards, C.G., Mao, R., 2003. Kinetics of chemical marker formation in whey protein gels for studying microwave sterilization. J. Food Eng. 60, 397–405.

Luan, D., Tang, J., Pedrow, P.D., Liu, F., Tang, Z., 2013. Using mobile metallic temperature sensors in continuous microwave assisted sterilization (MATS) systems. J. Food Eng. 119, 552–560.

Luan, D., Tang, J., Pedrow, P.D., Liu, F., Tang, Z., 2015. Performance of mobile metallic temperature sensors in high power microwave heating systems. J. Food Eng. 149, 114–122.

Mudgett, R.E., 1986. In: Rao, M.A., Rizvi, S.S.H. (Eds.), Electrical Properties of Foods. In Engineering Properties of Foods. Marcel Dekker, New York, pp. 329–390.

Pandit, R.B., Tang, J., Liu, F., Pitts, M., 2007. Development of a novel approach to determine heating pattern using computer vision and chemical marker (M-2) yield. J. Food Eng. 78, 522–528.

Pathak, S.K., Liu, F., Tang, J., 2003. Finite difference time domain (FDTD) characterization of a single mode applicator. J. Microw. Power Electromagn. Energy 38 (1), 1–12.

Rattanadecho, P., 2006. The simulation of microwave heating of wood using a rectangular wave guide: influence of frequency and sample size. Chem. Eng. Sci. 61, 4798–4811.

Resurrection, F.P., Tang, J., Pedrow, P., Cavalieri, R., Liu, F., Tang, Z., 2013. Development of a computer simulation model for processing food in a microwave assisted thermal sterilization (MATS) system. J. Food Eng. 118, 406–416.

Resurrection, F.P., Luan, D., Tang, J., Liu, F., Tang, Z., Pedrow, P., Cavalieri, R., 2015. Effect of changes in microwave frequency on heating patterns of foods in a microwave assisted thermal sterilization system. J. Food Eng. 150, 99–105.

Sadiku, M.N.O., 2007. Elements of Electromagnetics, fourth ed. Oxford, New York.

Sosa-Morales, M.E., Valerio-Junco, L., Lopez-Malo, A., Garcia, H.S., 2010. Dielectric properties of foods: reported data in the 21st century and their potential applications. LWT-Food Sci. Technol. 43, 1169–1179.

Tang, J., 2015. Unlocking potential of microwave energy for food safety and quality. J. Food Sci. 80, E1776–E1793.

Tang, Z., Mikhaylenko, G., Liu, F., Mah, J.H., Tang, J., Pandit, R., Younce, F., 2008. Microwave sterilization of sliced beef in gravy in 7 oz trays. J. Food Eng. 89 (4), 375–383.

Tang, J., Liu, F., Pathak, S., Eves, G., 2006. Apparatus and Method for Heating Objectives with Microwaves. U.S. Patent 7,119,313.

Wappling-Raaholt, B., Scheerlinck, Galt, S., Banga, J.R., Alonso, A., Balsa-Canto, Van Impe, J., Ohlsson, T., Nicolai, B.M., 2002. A combined electromagnetic and heat transfer model for heating of foods in microwave combination ovens. J. Microw. Power Electromagn. Energy 37 (2), 97–111.

Wang, Y., Tang, J., Rasco, B., Wang, S., Alshami, A.A., Kong, F., 2009. Using whey protein gel as a model food to study the dielectric heating properties of salmon (Oncorhynchus gorbuscha) fillets. LWT-Food Sci. Technol. 42, 1174–1178.